GED-0507 attenuates lung fibrosis by counteracting myofibroblast transdifferentiation in vivo and in vitro.

Silvia Speca, Caroline Dubuquoy, Christel Rousseaux, Philippe Chavatte, Pierre Desreumaux, P. Spagnolo

HAL Id: hal-04482627
https://hal.univ-lille.fr/hal-04482627v1

Submitted on 28 Feb 2024

PLOS ONE

GED-0507 attenuates lung fibrosis by counteracting myofibroblast transdifferentiation *in vivo* and *in vitro*

Silvia Speca[1]*, Caroline Dubuquoy[2], Christel Rousseaux[2], Philippe Chavatte[1,3], Pierre Desreumaux[1,4], Paolo Spagnolo[5]*

1 Univ. Lille, INSERM, U1286 –Infinite–Institute for Translational Research in Inflammation, Lille, France, 2 Intestinal Biotech Development, Lille, France, 3 Laboratoire de Pharmacie Clinique, Faculté des Sciences Pharmaceutiques et Biologiques, Lille, France, 4 Hepato-Gastroenterology Department, CHU Lille, Lille, France, 5 Respiratory Disease Unit, Department of Cardiac, Thoracic, Vascular Sciences and Public Health, University of Padova, Padova, Italy

* paolo.spagnolo@unipd.it (PS); silviaspeca@icloud.com (SS)

Abstract

The development of more effective, better tolerated drug treatments for progressive pulmonary fibrosis (of which idiopathic pulmonary fibrosis is the most common and severe form) is a research priority. The peroxisome proliferator-activated receptor gamma (PPAR-γ) is a key regulator of inflammation and fibrosis and therefore represents a potential therapeutic target. However, the use of synthetic PPAR-γ agonists may be limited by their potentially severe adverse effects. In a mouse model of bleomycin (BLM)-induced pulmonary fibrosis, we have demonstrated that the non-racemic selective PPAR-γ modulator GED-0507 is able to reduce body weight loss, ameliorate clinical and histological features of pulmonary fibrosis, and increase survival rate without any safety concerns. Here, we focused on the biomolecular effects of GED-0507 on various inflammatory/fibrotic pathways. We demonstrated that preventive and therapeutic administration of GED-0507 reduced the BLM-induced mRNA expression of several markers of fibrosis, including transforming growth factor (TGF)-β, alpha-smooth muscle actin, collagen and fibronectin as well as epithelial-to-mesenchymal transition (EMT) and expression of mucin 5B. The beneficial effect of GED-0507 on pulmonary fibrosis was confirmed *in vitro* by its ability to control TGFβ-induced myofibroblast activation in the A549 human alveolar epithelial cell line, the MRC-5 lung fibroblast line, and primary human lung fibroblasts. Compared with the US Food and Drug Administration-approved antifibrotic drugs pirfenidone and nintedanib, GED-0507 displayed greater antifibrotic activity by controlling alveolar epithelial cell dysfunction, EMT, and extracellular matrix remodeling. In conclusion, GED-0507 demonstrated potent antifibrotic properties and might be a promising drug candidate for the treatment of pulmonary fibrosis.

Introduction

Peroxisome proliferator-activated receptor-gamma (PPAR-γ) is a ligand-inducible nuclear transcription receptor that has a key role in organ homeostasis and downregulates inflammation and fibrosis [1–3]. Thanks to its broad regulatory activities and ability to bind a variety of natural or synthetic ligands, PPAR-γ is a potential therapeutic target in a range of inflammatory and fibrotic diseases [2, 4]. However, the majority of synthetic full PPAR-γ agonists are associated with serious adverse effects—possibly due to both their stereochemistry and their potential conversion into various metabolically active intermediates. Computational-chemistry-based studies have driven the development of highly efficacious small chiral nonracemic ligands that differentially activate PPAR-γ without inducing adverse effects. These compounds are referred to as selective PPAR modulators (SPPARMs).

The SPPARM (S)-(−)-GED-0507-34 (GED-0507) was developed as 5-aminosalycilate analog but has stronger PPARγ-mediated anti-inflammatory activity and a good safety/tolerability profile [4].

We have shown previously that GED-0507 exerts antifibrotic activity in a mouse model of bleomycin (BLM)-induced pulmonary fibrosis and in a mouse model of experimental dextran sodium sulfate (DSS)-induced intestinal inflammation [3]. Specifically, we demonstrated that GED-0507 reduced intestinal fibrosis in the DSS mouse model by inhibiting the TGFβ/Smad pathway, which is activated by persistent tissue injury and chronic inflammation. Consequently, several cytokines, growth factors and chemokines are produced in an uncontrolled manner, leading to the activation of myofibroblasts—a profibrotic cellular phenotype that expresses alpha-smooth muscle actin (αSMA). Myofibroblasts are derived from the transdifferentiation of several cell types, (including fibroblasts, epithelial cells, endothelial cells, and vascular smooth muscle cells) and synthesize large amounts of extracellular matrix (ECM) components. Excessive ECM deposition leads to parenchymal distortion and loss of function of the affected organ, and is a feature of all fibrotic diseases [5].

Pulmonary fibrosis is a frequent complication of interstitial lung disease (ILD), a large and heterogeneous group of conditions characterized by various degrees of inflammation and fibrosis [6]. Idiopathic pulmonary fibrosis (IPF) is the most common and severe form of ILD, with a median survival time from diagnosis is 3 to 5 years if untreated [7, 8]. According to current estimates, approximately 3 million people worldwide are affected by IPF. The 2015 guidelines on the treatment of IPF posed a conditional (i.e., weak) recommendation for the use of two drugs: pirfenidone (Pirf), a compound with anti-inflammatory, antioxidant and antifibrotic properties and nintedanib (Nint), an intracellular inhibitor of triple tyrosine kinases receptors, such as the vascular endothelial growth factor receptor 1–3, the fibroblast growth factor receptor 1–3, and the platelet-derived growth factor receptor a and b [9]. Pivotal clinical trials, systematic reviews and meta-analyses indicate for both drugs similar efficacy in slowing down functional decline and disease progression in IPF [10–12]. However, neither drug improves or even stabilizes lung function, and both have tolerability issues and significant discontinuation rates [13]. As such, there is high unmet need for more efficacious and better tolerated therapeutics [14].

The objectives of the present study were to characterize *in vivo* the biomolecular effects of GED-0507 in a murine model of BLM-induced pulmonary fibrosis and to evaluate *in vitro* its ability to prevent immortalized human epithelial cell and fibroblast lines and primary human lung fibroblasts (HLFs) from differentiating towards a pro-fibrotic profile [15–18].

Materials and methods

Animals and ethics statement

Eight-week-old C57BL/6 mice (n = 108) were purchased from Janvier Labs (Le Genest-Saint-Isle, France) and maintained in an accredited pathogen-free facility at the Pasteur Institute of Lille (Lille, France). Mice were provided with standard chow and ad libitum access to water. The mice were randomized to treatment with (A) PBS (n = 12), BLM (n = 22), BLM+GED-0507 (n = 20), and BLM+Pirf (n = 10) with preventive intent, and (B) PBS (n = 5), BLM (n = 10), BLM+ GED-0507 (n = 10), BLM+Nint (n = 10) and BLM+Pirf (n = 9) with curative intent. In order to ensure adequate statistical power, the sample size for each group was defined by considering the previously reported mortality rate induced by BLM administration [7]. Distress and body weight loss are clinical endpoints in the murine model of BLM-induced lung fibrosis, and so supportive care for minimizing these effects was not provided. However, the mice were observed daily for signs of distress and monitored weekly for body weight loss. All experiments were carried out in accordance with the European Directive No. 2010/63/EU, revising Council Directive No. 86/609/EEC of November 24, 1986 (number of ethic protocol: 2020061914271271). Animal handling and euthanasia were carried out by qualified personal for animal experimentation, in accordance with the French directive No. 2013–118 of 1st February 2013.

Compounds

BLM sulfate was purchased from Sigma Aldrich (Saint-Quentin-Fallavier, France), GED-0507 was purchased from PPM Services SA (Morbio Inferiore, Switzerland), Pirf was bought from TCI Europe N.V. (Boerenveldseweg, Belgium), and Nint came from Interchim (Kampenhout, Belgium).

Experimental design in mice

Lung fibrosis was induced in mice by a single intratracheal instillation of 0.8 mg/kg (0.025 U/kg) BLM. Starting on day 1 after BLM administration (for treatment with preventive intent) or day 14 (for treatment curative intent), mice were treated daily by oral gavage with optimal concentrations of GED-0507 (100 mg/Kg/day), Pirf (400 mg/Kg/day) or Nint (60 mg/Kg/day) dissolved in 0.5% carboxymethylcellulose + 1% v/v Tween 80. The direct effects of each compound tested were observed 28 days after the BLM administration. The study design is summarized in S1 Fig.

After excision, left lungs were fixed in 4% buffered formaldehyde and embedded in paraffin for histological analysis, whereas right lungs were dissected and stored at -80˚C for molecular analysis.

A549 and MRC-5 cell lines and primary HLFs

A549 (ATCC® CCL-185™, Molsheim Cedex, France) and MRC-5 (ATCC® CCL171™) cell lines were grown in Dulbecco's modified Eagle's medium supplemented with 100 U/ml penicillin, 100 μg/ml streptomycin and 10% fetal bovine serum (FBS). HLFs (ATCC® PCS-201-013™, *Homo Sapiens*, Normal Lung) were grown in Fibroblast Basal Medium (ATCC® PCS-201-030™) supplemented with 100 U/ml penicillin, 100 μg/ml streptomycin and a Fibroblast Growth Kit-Low serum (ATCC® PCS-201-041™), according to the manufacturer's instructions. Cells were maintained in a humidified atmosphere with 95% air and 5% CO_2 at 37˚C. For each cell type, myofibroblast differentiation was obtained by incubation with human

recombinant TGFβ1 (T7039, Sigma Aldrich, Saint-Quentin-Fallavier, France) at optimal concentrations of 20 ng/ml for A549 cells, 10 ng/mL for MRC-5 cells, and 5 ng/mL for HLFs.

The cell viability assay

Cell viability was measured using an MTT assay (CellTiter 96® Non-Radioactive Cell Proliferation Assay, Promega, Charbonnieres Les Bains, France), according to the manufacturer's instructions. A549 cells, MRC-5 cells and HLFs were exposed to growing concentrations of GED-0507 (0.1, 1, 10, and 30 mM), Pirf (0.1, 0.4, 0.8, and 1.6 mM) and Nint (0.1, 0.5, 1, and 10 μM) over 2, 4 or 6 days. Pirf and Nint were dissolved in dimethyl sulfoxide (DMSO) (D4540, Sigma Aldrich), ensuring that the concentration of DMSO in the treatment medium did not exceed 1% v/v. The optimal *in vitro* doses of GED-0507, Pirf and Nint were selected after time- and dose-dependent investigations in each cell line, in order to modulate the main fibrotic pathways without reducing cell viability [2, 19, 20].

Picrosirius red staining

Collagen deposition was determined by picrosirius red staining of paraffin-embedded lung sections or cultured cells. Briefly, 4 μm dried tissue sections or monolayers of 2%-paraformaldehyde (PFA)-fixed A549 and MRC-5 cells were stained with 0.1% direct red stain (365548, Sigma Aldrich)/0.5% picric acid (36011, Sigma Aldrich) for 1 h at room temperature (picrosirius red staining) [21]. Each slide was examined and analyzed remotely using Image J software (W.S. Rasband, National Institutes of Health, Bethesda, MD; http://rsb.info.nih.gov/ij/, 1997–2011), and the mean staining intensity was quantified with the threshold detection method on grayscale images taken from three different microscope fields (magnification: x20).

For cell monolayers, bound picrosirius red was eluted by incubation for 1 h at 37˚C with 0.1 N NaOH. Solubilized dye was recovered after each treatment and the absorbance was measured at 550 nm. The results were normalized against the cell density in the remaining monolayers after staining with the DNA-binding dye Crystal Violet for 30 min at room temperature. After elution with pure methanol, the dye's absorbance at 540 nm was measured [22].

α-SMA immunofluorescent staining

α-SMA protein expression on 4-μm fixed lung sections and in cell lines (A549 and MRC-5 cells) was evaluated using an immunofluorescence assay. Briefly, after permeabilization in 0.1% Triton-X 100, lung sections and cells were incubated overnight at 4˚C with a polyclonal anti-α-SMA primary antibody (ab5694, Abcam, Paris, France) at the dilution of 1:200. Subsequently, the samples were incubated with a specific conjugated anti-mouse secondary antibody AlexaFluor 488 (A32723, ThermoFisher Scientific, Illkirch Cedex, France) for 1 h at room temperature. Nuclei were stained with Hoechst 33342 dye (62249, ThermoFisher Scientific). The staining was quantified using Image J software and the threshold detection method on grayscale images taken from three different microscope fields (magnification: x20/x40) [23]. Data were expressed as fold change in the mean ± standard error of the mean (SEM) staining intensity/total area for the treatment group vs. the control group.

Quantitative RT-PCRs

Gene expression levels of pro-fibrotic markers (such as TGFβ, α-SMA, collagen, and fibronectin) were measured in lung tissues, cell lines, and HLFs using quantitative real time polymerase chain reactions (qPCRs). The mRNA levels of pro-inflammatory cytokines (such as the interleukin (IL)-1β and the tumor necrosis factor (TNF)-α) epithelial cell markers (E-cadherin and

occludin) and mucins (MUC5B) were also measured. Briefly, mRNA was extracted using an RNA purification kit from Macherey-Nagel (Hœrdt, France) and reverse-transcribed to cDNA. The qPCRs were run on a Light Cycler FastStart DNA Master SYBR Green I system (4385617, ThermoFisher Scientific), according to the manufacturer's instructions. The primers' sequences and NCBI references are listed in S1 and S2 Tables. Relative gene expression was calculated as E = $2^{-\Delta Ct}$, where ΔCt is the difference between the critical threshold cycle (Ct) values of each gene and the relative Ct of GAPDH. Data were expressed as the fold change in the mean ± SEM relative gene expression value for the treatment group vs. the control group.

Western blotting

Protein expression levels of α-SMA, collagen and fibronectin were determined by Western blotting of HLF extracts. Briefly, total proteins were extracted using RIPA buffer (R0278, Sigma Aldrich, Saint-Quentin-Fallavier, France) supplemented with 100 mM sodium fluoride, 2 mM sodium orthovanadate, 2 mM sodium pyrophosphate, 1 mM phenylmethylsulphonyl fluoride (Sigma Aldrich) and a standard protease inhibitor cocktail (11836170001, Sigma Aldrich). 50 μg of total protein from each sample were separated by SDS-PAGE electrophoresis using Novex Tris-glycine gels with polyacrylamide gradients ranging from 4 to 12% (Novex™ 4–12% Tris-Glycine Mini Gels, 15-well WedgeWell™, ThermoFisher Scientific) and then transferred onto nitrocellulose membranes using the iBlot 2 Dry Blotting System (ThermoFisher Scientific). The membranes were immunoblotted with specific monoclonal antibodies against α-SMA (67735, Proteintech, Manchester, United Kingdom) at dilution of 1:1000 (overnight at 4˚C), collagen (66761, Proteintech) at dilution of 1:1000 overnight at 4˚C), fibronectin (66042, Proteintech) at dilution of 1:1000) or β-actin (A5441, Sigma Aldrich) at dilution of 1:10000 (2 h at room temperature). Next, blots were incubated with a secondary anti-rabbit horseradish-peroxidase-conjugated antibody (A6154, Sigma Aldrich) at dilution of 1:10000 for 1 h at room temperature and revealed with chemiluminescent substrate (Immobilon ECL Ultra Western HRP Substrate, Sigma Aldrich), according to the manufacturer's instructions. The membranes were exposed to autoradiography films (Hyperfilm ECL, ThermoFisher Scientific), and the optical density of target bands was determined using a computer-assisted densitometer and ImageJ software. Protein levels were expressed in optical density units per quantity of total protein. The values for each protein were normalized against the internal control (β-actin) in each sample.

Statistical analysis

Groups were compared using a Kruskal-Wallis non-parametric analysis of variance. Post-hoc comparisons of pairs of groups were performed using the Wilcoxon rank sum test. Data were expressed as the mean ± SEM. The threshold for statistical significance was set to $p < 0.05$.

Results

In vivo experiments

mRNA expression levels of pro-inflammatory cytokines. One of the main consequences of BLM treatment is the activation of an early inflammatory response, which is maintained over time. We therefore initially evaluated the mRNA expression levels of pro-inflammatory cytokines. Firstly, we found that the lung expression levels of *Tnf* (the gene encoding TNF-α) and *Il1b* (the gene encoding IL-1β) were higher in BLM-treated mice than in control animals (Fig 1). The preventive administration of GED-0507 and Pirf downregulated the pro-
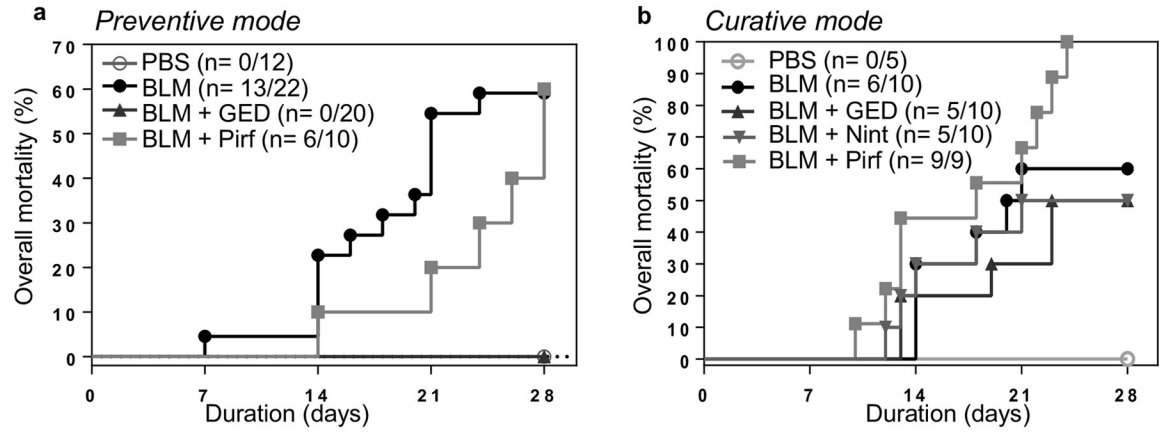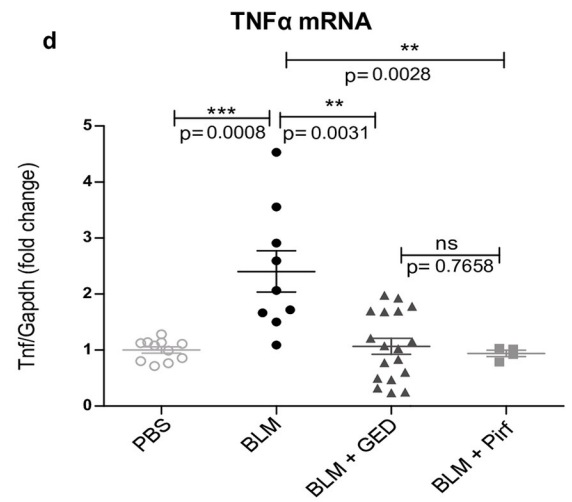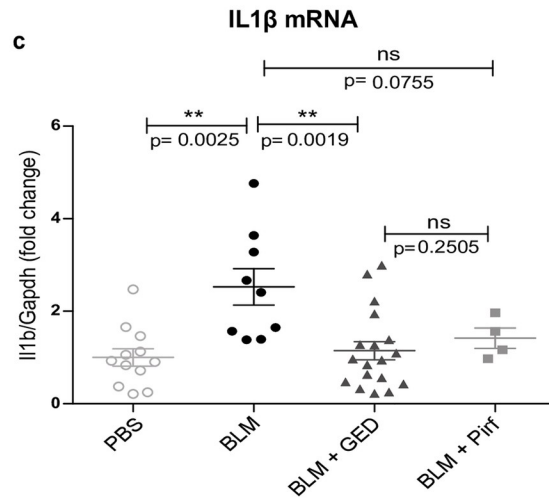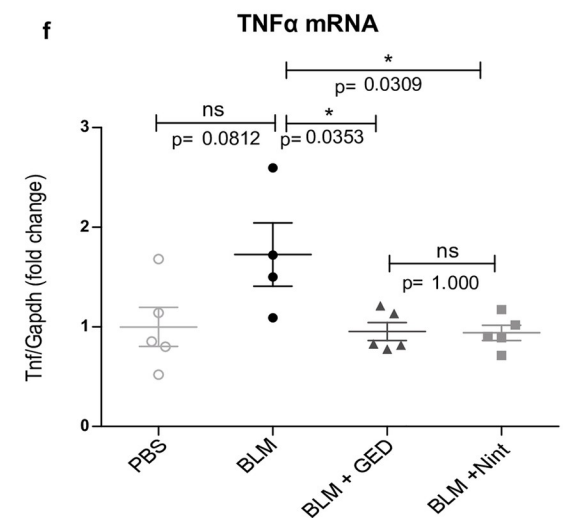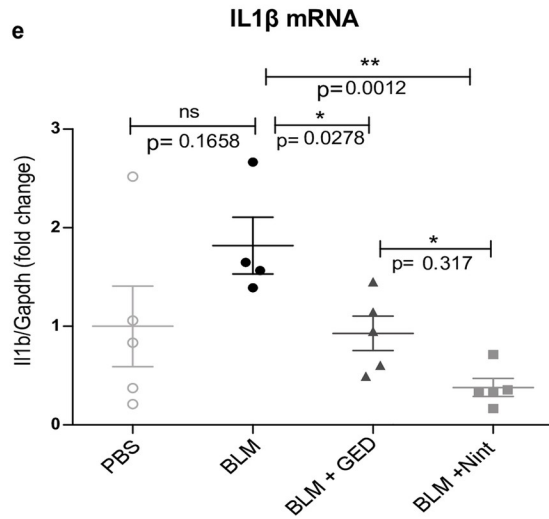
Fig 1. Pro-inflammatory cytokines following the administration of GED-0507, Pirf or Nint with preventive or curative intent. The original groups sizes in the preventative study were n = 12 for PBS, n = 22 for BLM, n = 20 for BLM+GED and n = 10 for BLM+Pirf groups. In the curative study mice were randomized to: PBS (n = 5), BLM (n = 10), BLM+GED (n = 10), BLM+Nint (n = 10) and BLM +Pirf (n = 9). (a,b) Kaplan-Meier curves depicting percent mortality versus time post-BLM. Consistent with our previous report, BLM administration causes 60% mortality rate (13/22 in the preventive study and 6/10 in the curative study). (a) When administered with preventive intent, 100% of GED-receiving mice survives, whereas Pirf treatment is associated to 60% mortality rate. (b) Curative treatments with GED and Nint cause 50% mortality rate (n = 5/10), whereas Pirf administration is associated with 100% mortality at day 24. All survivors are analyzed and reported here. (c-f) Dot plots depicting mRNA expression levels of pro-inflammatory cytokines, (c, e) *Tnf* and (d, f) *Il1b*, measured using quantitative RT-PCR, in frozen lungs of surviving mice after drug administration with preventive or curative intent. The data are quoted as the mean ± SEM fold change vs. PBS-treated mice. * = p< 0.05; ** = p< 0.01; *** = p< 0.001; ns = not significant.

inflammatory gene profile in BLM-treated mice (Fig 1C and 1D). When administered on a curative basis, both GED-0507 and Nint significantly decreased the transcriptional upregulation of *Tnf* and *Il1b* induced by BLM (Fig 1E and 1F). In line with previous observations, curatively administered Pirf resulted in a mortality rate of 100% at day 24, making any further evaluation of the mechanisms and molecular parameters of lung fibrosis unfeasible (Fig 1B) [24].

Evaluation of mRNA and protein levels of lung fibrosis markers. In preliminary experiments, we assessed the ability of GED-0507 to reduce weight loss, mortality rate, lung macroscopic lesions, and histological parameters in BLM-treated mice [25]. Here, we performed a more detailed analysis of biomolecular mechanisms related to GED-0507 capacity to control lung fibrosis.

The pulmonary expression of all tested genes—*Tgfb1* (coding for TGFβ), *Acta2* (coding for α-SMA), *Col1a1* (coding for collagen) and *Fn1* (coding for fibronectin)—was greater in the BLM-treated mice than in control animals (Figs 2 and 3). Preventive administration of GED-0507 significantly downregulated the BLM-induced mRNA expression of all these markers, with Pirf exerting a similar but less pronounced effect (Fig 2A, 2B, 2E and 2H). GED-0507 also exerted an inhibitory effect on the protein expression of the myofibroblast differentiation marker α-SMA, as observed and quantified in an immunofluorescence assay (Fig 2C and 2D). Protein expression levels of collagen were also lower after treatment with GED-0507, as observed via picrosirius red staining and its relative quantification with digital imaging. Conversely, relative to control BLM-treated animals, preventive treatment with Pirf significantly decreased collagen deposition only (Fig 2F and 2G). Along with the elevated expression of major fibrosis markers, we also observed modulation of the BLM-induced pulmonary epithelial signature. Indeed, the lung tissue expression of genes coding for epithelial cell markers (such as *Cdh1* coding for E-cadherin and *Ocln* coding for occludin) was significantly lower in BLM mice than in control animals. Preventive treatment with GED-0507 restored the loss of E-cadherin and occludin to levels similar to those measured in the lungs of PBS-treated mice. Conversely, Pirf did not prevent the BLM-induced decrease of either E-cadherin or occludin mRNA levels (Fig 2I and 2J). We also found that mRNA expression of MUC5B (encoded by *Muc5b)* in the lung was significantly greater in BLM-treated mice than in control animals. Preventive treatment with GED-0507 was associated with a significantly lower level of transcriptional expression of *Muc5b* in BLM-treated mice, whereas no significant effect was observed in mice receiving Pirf (Fig 2K).

When GED-0507 and Nint were given with curative intent (Fig 3), both compounds were not able to reduce the *Tgfb1* expression levels, nevertheless GED-0507 and Nint were associated with significantly and similarly low levels of *Acta2*, *Col1a1*, *Fn1* transcription (Fig 3A, 3B, 3E and 3H). This transcriptional effect translated into significantly lower levels of protein expression of α-SMA and collagen in mice with lung fibrosis receiving GED-0507 or Nint with

Fig 2. Biomolecular parameters following the administration of GED-0507, Pirf or Nint with preventive intent. For explanation of group size, refer to Fig 1. (a, b, e and h) The dot plots depict mRNA expression levels of *Tgfb*, *Acta2*, *Col1A1* and *Fn1* in frozen lung, as quantified in RT-PCRs. (c) Microphotographs of immunofluorescence staining of α-SMA (green), at a magnification of 40x. Nuclei were counterstained using DAPI (blue). Digital images were processed with the Zeiss LSM Browser, and α-SMA protein expression was quantified on three microscope fields, using the threshold detection method. (d) Scatter plot of α-SMA quantification. (f) Microphotographs of picrosirius red staining on lung sections, for collagen fibers. Images were scanned at a magnification of 40x, and collagen deposition (red) was quantified on digitized images and (g) plotted. (i, j) The loss of epithelial cell markers reflects the pro-fibrotic EMT. Scatter plots show the mRNA expression of epithelial cell markers *Cdh1* and *Ocln*, quantified in RT-PCRs on frozen lungs of all surviving mice. (k) Dot plots depicting mRNA expression levels of *Muc5b*. Data are quoted as the mean ± SEM fold change vs. PBS-treated mice; * = p< 0.05; ** = p< 0.01; *** = p< 0.001; ns = not significant.

https://doi.org/10.1371/journal.pone.0257281.g002

curative intent, relative to untreated animals (Fig 3C, 3D, 3F and 3G). In this context, GED-0507 (but not Nint) also attenuated the BLM-induced decrease in *Cdh1* expression, whereas no effect was observed with regard to *Ocln* (Fig 3I and 3J). Compared to BLM-treated mice, gene expression levels of *Muc5B* were also significantly lower following administration of GED-0507 or Nint with curative intent (Fig 3K).

In vitro experiments

Cell viability. In order to determine *in vitro* toxicity, we exposed three types of cell to GED-0507, Pirf and Nint. For GED-0507, the results of the cell toxicity assay showed that none of the doses used in the present experiments were cytotoxic after 2, 4 and 6 days of exposure. Conversely, cytotoxic effects were observed in A549 and MRC-5 cell lines treated with
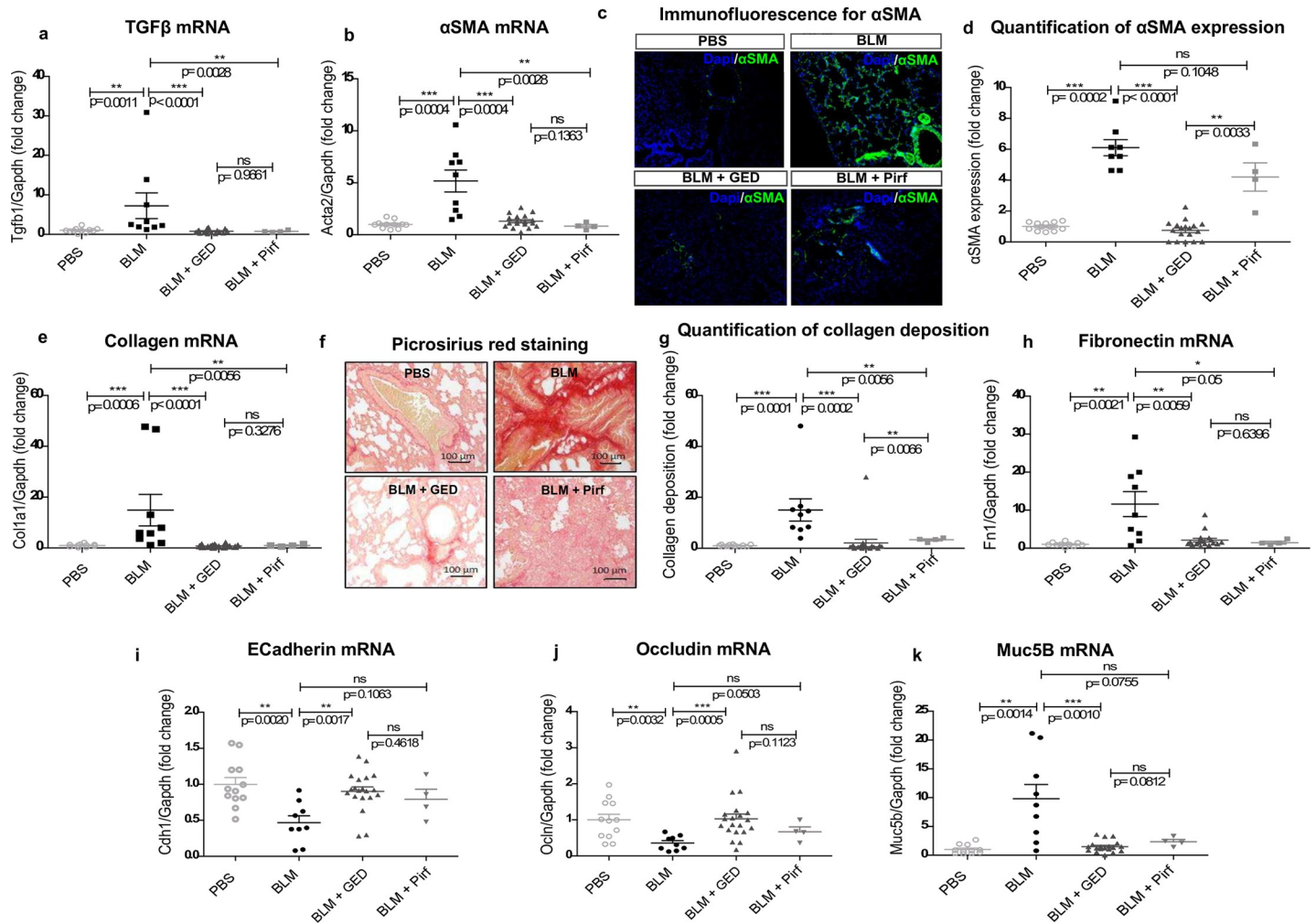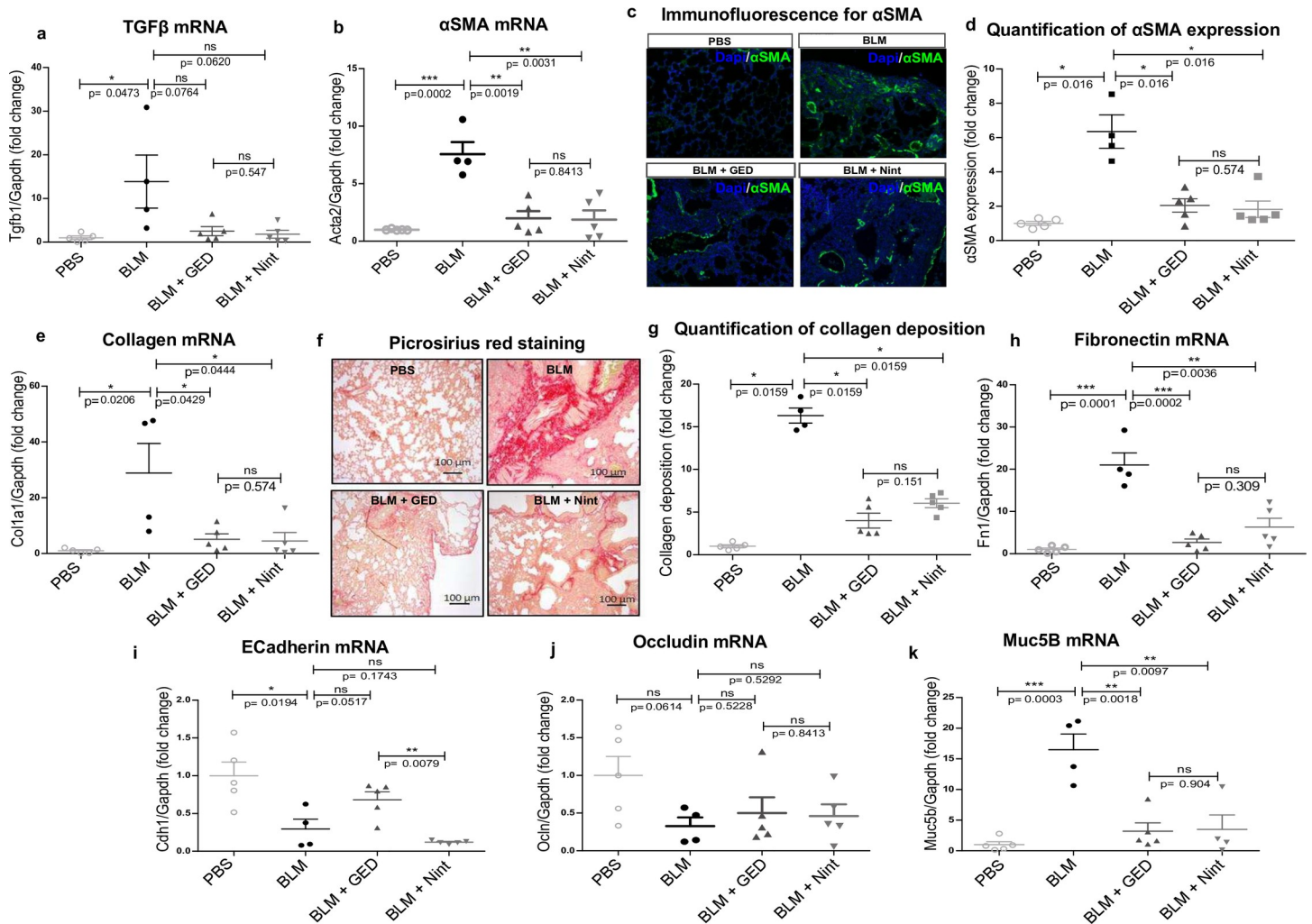
Fig 3. Biomolecular parameters following the administration of GED-0507 and Nint with curative intent. For explanation of group size, refer to Fig 1. (a, b, e and h) Dot plots depicting mRNA expression levels of *Tgfb*, *Acta2*, *Col1A1* and *Fn1* genes quantified in frozen lung in RT-PCRs. (c) Microphotographs of immunofluorescence staining of α-SMA (green) scanned at a magnification of 40x. Nuclei were counterstained using DAPI (blue). Digital images were processed with the Zeiss LSM Browser, and α-SMA protein expression was quantified on three microscope fields, using the threshold detection method. (d) Scatter plot for α-SMA quantification. (f) Microphotographs of picrosirius red staining of lung sections, for collagen fibers. Images were scanned at a magnification of 40x, and collagen deposition (red) was quantified on digitized images and (g) plotted. (i, j) The loss of epithelial cell markers reflects the pro-fibrotic EMT. Scatter plots show the mRNA expression of epithelial cell markers *Cdh1* and *Ocln*, quantified in RT-PCRs on frozen lungs of all surviving mice. (k) Dot plots depicting mRNA expression levels of *Muc5b*. Data are quoted as the mean ± SEM fold change vs. PBS-treated mice. * = p< 0.05; ** = p< 0.01; *** = p< 0.001; ns = not significant.

the highest concentration of Nint (i.e., 10 μM) and Pirf (i.e., 1.6 μM) on day 2 and day 4, respectively. Based on our time- and dose-dependent assessments of the viability of MRC-5 and A549 cells over two and four days, respectively, the optimal doses were found to be 1–30 mM in 2% FBS culture medium for GED-0507, 0.1–1 μM in 0.2% FBS culture medium + 0.01% DMSO for Nint, and 0.1–0.8 mM + 0.01% DMSO for Pirf. In terms of viability, HLFs were more sensitive to Pirf and Nint than MRC-5 and A549 cells were. Indeed, a cytotoxic effect was observed after 2 days of incubation with Pirf and Nint at doses of 0.8 mM and 1 μM, respectively. The highest tolerated non-cytotoxic concentrations were 0.4 mM and 0.5 μM for Pirf and Nint, respectively, after a maximum stimulation time of 2 days. Therefore, a study design including two days of incubation with GED-0507 (1–30 mM), Nint (0.1–0.5 μM) and Pirf (0.1–0.4 mM) was applied to HLFs (S2 Fig).

Evaluation of the ability of GED, Nint and Pirf to counter TGFβ-induced myofibroblast activation in the MRC-5 lung fibroblast cell line. The fibroblast-to-myofibroblast transition in MRC-5 cells was induced by 10 ng/mL TGFβ stimulation over two days, leading to a significant elevation in expression of the main fibrosis markers at both the mRNA and protein levels (Fig 4). At a concentration of 1 mM, GED-0507 was able to counter the TGFβ-induced upregulation of *TGFB1* expression. The TGFβ-induced expression of all the other tested profibrotic genes (such as *ACTA2*, *COL1A1*, and *FN1*) was equally reduced by both doses of GED-0507 (1 and 30 mM). Conversely, the expression of these genes was not significantly modulated when MRC-5 cells were treated with Pirf or Nint under the same conditions (Fig 4A–4D).

Furthermore, GED-0507 was able to exert an inhibitory effect on α-SMA and collagen protein expression, as observed and quantified in an immunofluorescence assay and picrosirius red staining, respectively (Fig 4E and 4G). Pirf was able to reduce TGFβ-induced collagen deposition but not the α-SMA protein expression (Fig 4G). The discrepancy between the mRNA and protein expression levels for collagen in Pirf-treated cells is consistent with the fact that the mRNA expression is related specifically to collagen I (the *COL1A1* gene) whereas picrosirius red stains all subtypes of collagens deposed by the cell.
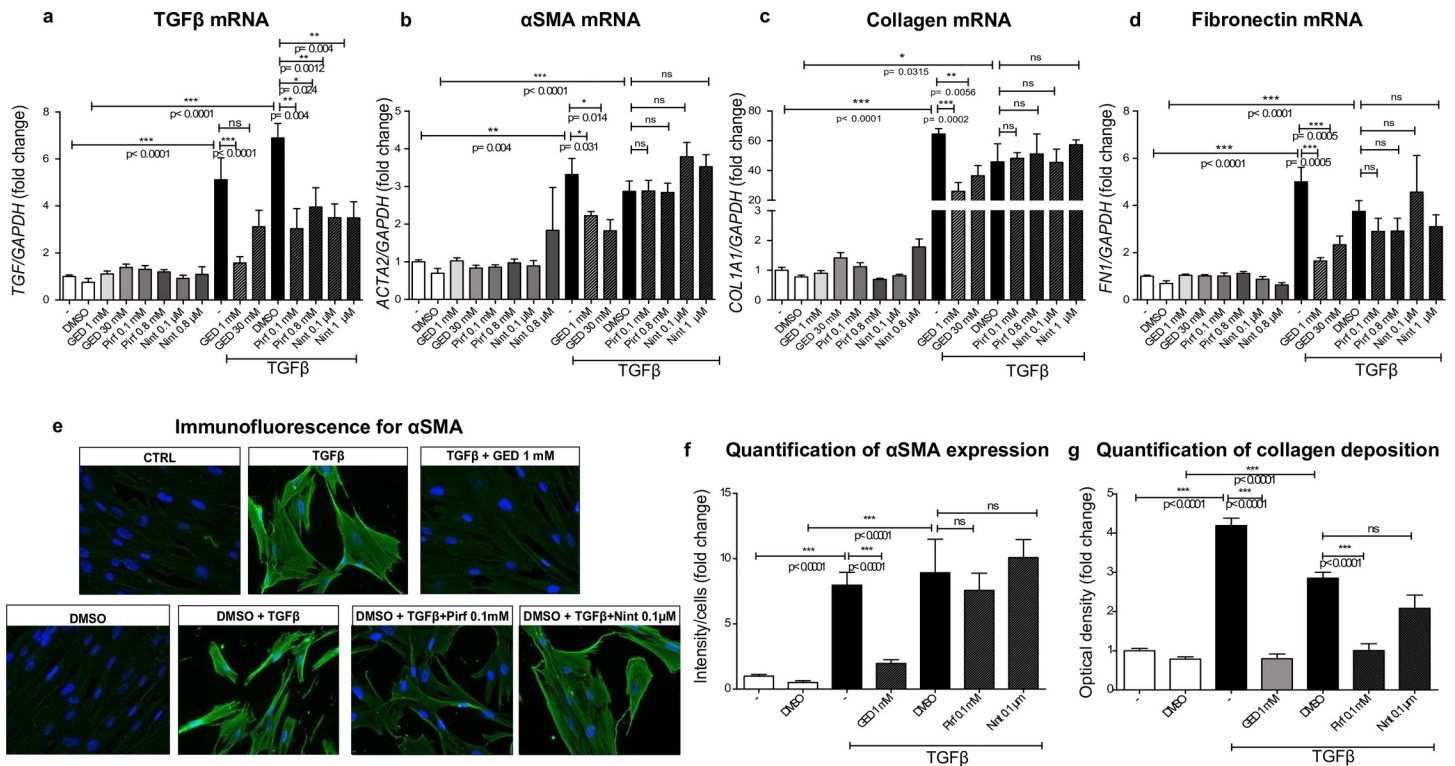
Fig 4. *In vitro* evaluation of myofibroblast activation in MRC-5. Myofibroblast activation was induced in MRC-5 human fibroblasts stimulated with 10 ng/mL TGFβ over two days. GED-0507 (1–30 mM), Pirf (0.1–0.8 mM) or Nint (0.1–1 μM) were administered at the same time as TGFβ. mRNA expression levels for (a) *TGFB1*, (b) *ACTA*, (c) *COL1A1* and (d) *FN1* were quantified in RT-PCRs and converted into histograms for three independent experiments performed in triplicate. (e) Microphotographs of immunofluorescence staining of α-SMA (green) were scanned at a magnification of 40x. Nuclei were counterstained using DAPI (blue). Digital images were processed with the Zeiss LSM Browser and (f) α-SMA protein expression was quantified on 3 microscope fields, using the threshold detection method with Image J software and represented on relative scatter plots. (g) Collagen deposition was quantified by picrosirius red staining and converted into histograms for 3 independent experiments performed in triplicate. Since Pirf and Nint were solubilized in DMSO, DMSO- and/or TGFβ+DMSO-treated cells were used as comparators in the statistical analysis. Data are quoted as the mean ± SEM fold change vs. CTRL cells. * = p< 0.05; ** = p< 0.01; *** = p< 0.001.

https://doi.org/10.1371/journal.pone.0257281.g004
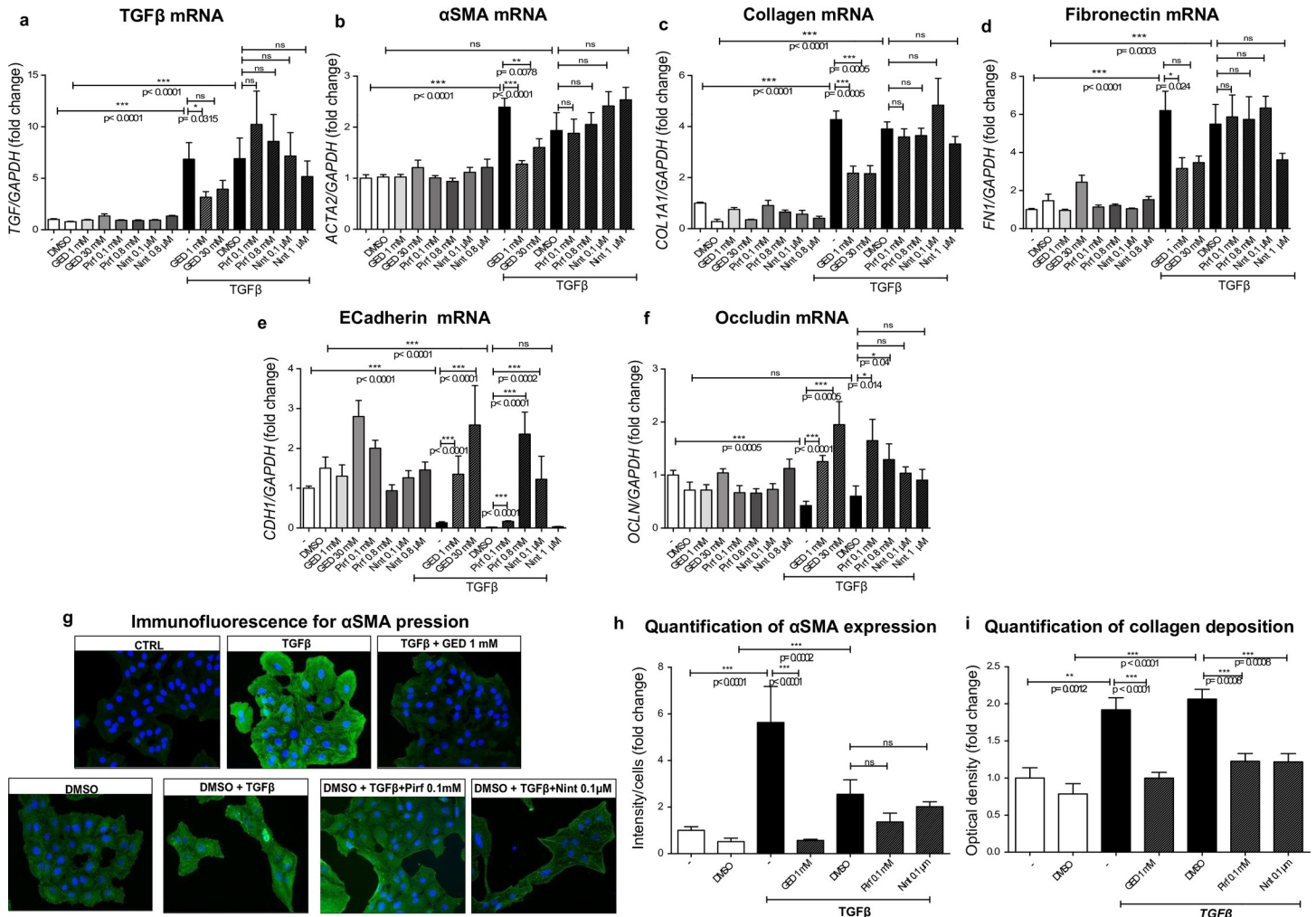
Fig 5. *In vitro* evaluation of the EMT in A549 cells. (a) Experimental scheme. The EMT was induced in human alveolar epithelial cells (A549) stimulated with 20 ng/mL TGFβ over four days. GED-0507 (1–30 mM), Pirf (0.1–0.8 mM) or Nint (0.1–1 μM) were administered at the same time of TGFβ stimulation. mRNA expression levels for mesenchymal cell markers (a) *TGFB1*, (b) *ACTA*, (c) *COL1A1*, (d) *FN1* and epithelial cell markers (e) *CDH1* and (f) *OCLN* were quantified in RT-PCRs and converted into histograms in 3 independent experiments performed in triplicate. (g) Microphotographs of immunofluorescence staining of α-SMA (green) were scanned at a magnification of 40x. Nuclei were counterstained using DAPI (blue). Digital images were processed with the Zeiss LSM Browser and (h) α-SMA protein expression was quantified on 3 microscope fields, using the threshold detection method with Image J software and represented on relative scatter plots. (i) Collagen deposition was quantified by picrosirius red staining and converted into histograms in 3 independent experiments performed in triplicate. Since Pirf and Nint were solubilized in DMSO, DMSO- and/or TGFβ+DMSO-treated cells were used as comparators in the statistical analysis. Data are quoted as the mean ± SEM fold change vs. CTRL cells. * = p< 0.05; ** = p< 0.01; *** = p< 0.001.

Evaluation of the ability of GED, Nint and Pirf to counter the TGFβ-induced mesenchymal transition in alveolar epithelial cells (A549). We next evaluated the expression of epithelial fibrosis markers in a monolayer of A549 cells (Fig 5). Four days of treatment with 20 ng/mL TGFβ over four days was associated with an increase in mRNA expression of *TGFB1*, *ACTA2, COL1A1* and *FN1*, and a decrease in mRNA expression of the genes coding for E-cadherin (*CDH1*) and occludin (*OCLN*). GED-0507 was able to restore the expression of all these genes to control levels, whereas Pirf and Nint reduced the overexpression of *TGFB* only (Fig 5A–5F). With regard to epithelial cell markers, Pirf (but not Nint) was able to restore mRNA levels of E-cadherin and occludin (Fig 5E and 5F).
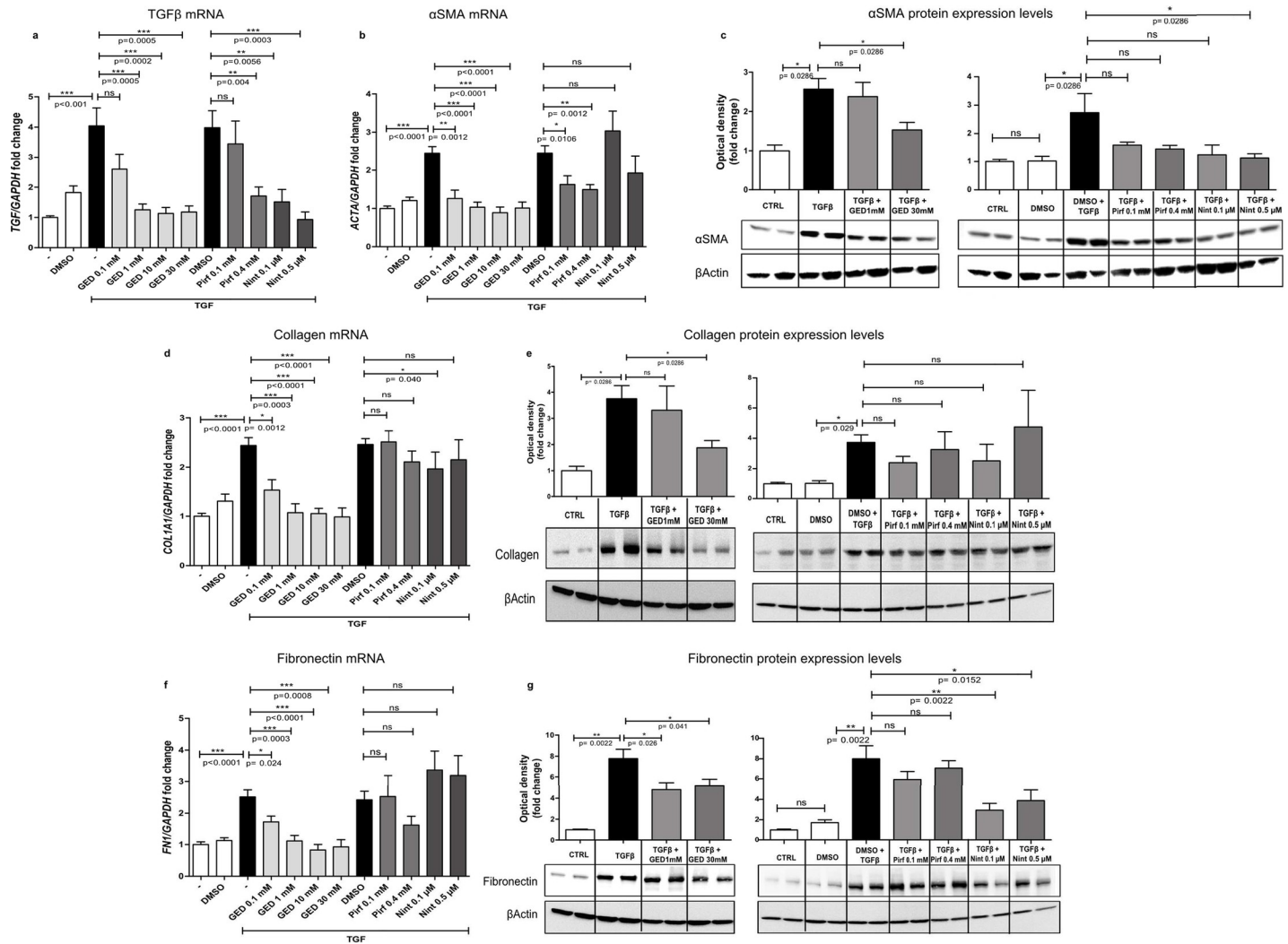
Fig 6. *In vitro* evaluation of myofibroblast activation in HLFs. Experimental plan. Myofibroblast activation was induced in primary human fibroblasts (HLFs) stimulated with 5 ng/mL TGFβ over two days. GED-0507 (1–30 mM), Pirf (0.1–0.4 mM) or Nint (0.1–0.5 μM) were administered at two different doses at the same time of TGFβ. mRNA expression levels for (a) *TGFB1*, (b) *ACTA*, (d) *COL1A1* and (f) *FN1* were quantified in RT-PCRs and converted into histograms for 3 independent experiments performed in triplicate. Protein expression levels for (c) α-SMA, (e) collagen and (g) fibronectin were evaluated on Western blots. Band density was quantified using ImageJ software and converted into histograms for 3 independent experiments in duplicate. Since Pirf and Nint were solubilized in DMSO, DMSO- and/or TGFβ+DMSO-treated cells were used as comparators in the statistical analysis. Data are quoted as the mean ± SEM fold change vs. CTRL cells. * = p< 0.05; ** = p< 0.01; *** = p< 0.001.

https://doi.org/10.1371/journal.pone.0257281.g006

Protein levels of α-SMA were significantly elevated in TGF-β-treated A549 cells. Collagen production (as measured by the optical density of the picrosirius red staining) was also enhanced. All three tested compounds were able to downregulate the TGF-β-induced post-transcriptional upregulation of α-SMA and collagen (Fig 5G and 5I). However, at both concentrations tested, the effect of GED-0507 was significantly greater than that of Pirf or Nint.

Evaluation of the ability of GED, Nint and Pirf to counter TGFβ-induced myofibroblast activation in primary HLFs. The fibroblast-to-myofibroblast transition in HLFs was induced by stimulation with 5 ng/mL TGFβ over two days (Fig 6). Starting at a concentration of 1 mM, all doses of GED-0507 were able to significantly decrease the expression of *TGFB1*, *ACTA2*, *COL1A1* and *FN1* genes, when compared with control TGFβ-stimulated cells. Pirf exerted only a limited inhibitory effect on *TGFB1* and *ACTA* genes, whereas Nint decreased

TGFB1 and *COL1A1* gene expression significantly when compared with TGFβ+DMSO-stimulated HLFs (Fig 6A, 6B, 6D and 6F). In Western blots, TGFβ-induced protein expression of α-SMA, collagen and fibronectin was also significantly reduced by 30 mM GED-0507. In contrast, Pirf was not able to reduce the post-transcriptional expression of all fibrosis markers, whereas Nint only reduced α-SMA and fibronectin protein levels at a higher concentration (0.5 μM) (Fig 6C, 6E and 6G).

Discussion

As seen in other organs, fibrosis of the lung is characterized by the excessive deposition of ECM components. When this deposition is extensive, it can lead to parenchymal distortion and irreversible loss of function [26]. IPF is the prototypical, progressive, fibrotic lung disease, with a dismal prognosis and no cure. Although evidence-based guidelines on the treatment of IPF recommend the use of Pirf and Nint, these drugs only reduce the rate of functional decline or disease progression, and are associated with tolerability issues [27–29].

The TGFβ/SMAD pathway has a central role in the differentiation of fibroblasts to myofibroblasts, persistent myofibroblast activation, and aberrant ECM deposition that result in tissue fibrosis [30]. However, owing to TGFβ's pleiotropic effects, abrogation of the TGFβ pathway may not be an ideal strategy. Instead, it might be more effective to focus on pathways directly associated with TGFβ in either an agonistic or antagonistic context (such as IL-13 or PPAR-γ, respectively). The nuclear receptor PPAR-γ is naturally activated by prostaglandins (PG)-D1 and PG-D2) and the PG derivative 15-deoxy-Δ12 and 15d-PGJ2, and a target of several synthetic ligands. PPARγ is expressed in a wide range of tissues, including colon, spleen, retina, skeletal muscle, liver and lung. A better understanding of the many biological effects of ligand-dependent PPAR-γ activation has led to the widespread clinical use of synthetic PPAR-γ ligands, such as thiazolidinediones (TZDs) [31]. The ability of TZDs (especially rosiglitazone) to regulate the production of several inflammatory mediators (e.g., TNFα, IL-6, MCP1, and PAI-1) in a number of pathological conditions suggests that PPAR-γ exerts similar anti-inflammatory effects. Natural PPAR-γ ligands (e.g. 15d-PGJ2) and synthetic PPAR-γ ligands (e.g. rosiglitazone) also have antifibrotic effects [32]. Burgess et al. have shown that PPAR-γ agonists are able to modulate the differentiation of human lung primary fibroblasts into myofibroblasts following the addition of exogenous TGFβ [33]. PPAR-γ ligands (mainly the TZDs) are also able to (i) facilitate tissue regeneration and the resolution of fibrosis in murine models of BLM-induced lung fibrosis [32, 34–36], and (ii) prevent radiation-induced pulmonary fibrosis [37]. The beneficial effect of PPARγ activation in controlling lung fibrosis may be due to the receptor's broad cellular distribution within the lung. Indeed, PPAR-γ are expressed by alveolar epithelial cells, fibroblasts, bronchial smooth muscle cells, type II pneumocytes, macrophages, endothelial cells, lymphocytes, and dendritic cells. PPAR-γ's functions depending on the cell type, which thus contributes to tissue homeostasis [38]. Conversely, the mechanisms underlying the antifibrotic properties of PPAR-γ activation in the lung remain to be elucidated. Despite their widespread use, full PPAR-γ agonists (such as the TZDs) are nevertheless associated with potentially serious adverse events [39]. However, PPAR-γ in the lung can be activated by a wide spectrum of compounds; these include SPPARMs, which induce specific conformational changes and thus resulting in differential activation and interactions with cofactors and corepressors. This strategy can avoid the adverse events associated with full agonists.

GED-0507 is a new SPPARM that binds with high affinity to the receptor's ligand binding domain, as predicted by docking simulations [4]. We have previously shown that GED-0507 exhibits potent anti-inflammatory and antifibrotic properties and has a good safety and

tolerability profile, thanks to its limited interference with lipid and glucose metabolism [2, 40, 41]. The latter effect has been demonstrated in studies of animals receiving very high oral doses of GED-0507 (including chronic toxicity studies in rats and in dogs, in which high systemic exposure to GED-0507 was achieved), and in Phase I and Phase II clinical studies of patients with inflammatory bowel disease [28]. GED-0507 also displays good absorption in the small intestine and significant retention in the lung. With regard to its biological activities, GED-0507 increases the expression of IkBα and thus preventing the nuclear translocation of NF-kB via transrepression [41]. Furthermore, we previously showed that exposure to GED-0507 counters the expression of genes coding for major profibrotic mediators (i.e., IL13 and the TGFβ/SMAD3 pathway), α-SMA and ECM components in mice with chronic intestinal inflammation [3]. In this context, GED-0507 appears to exert its antifibrotic effects through several mechanisms, including PPAR-γ activation and thus the maintenance of intestinal epithelial homeostasis and modulation of the epithelia-to-mesenchymal transition and the EMT [24, 42, 43].

The present study follows up on earlier work in which we showed that prophylactic oral administration of GED-0507 at the optimal dose of 100 mg/kg/day abolished the excessive mortality and weight loss observed three weeks after BLM administration in non-treated animals (24). When given with curative intent, GED-0507 reduced the mortality rate among mice receiving BLM by 50% and was associated with a weight gain similar to that seen in PBS-treated control animals without lung fibrosis. In BLM-treated mice, macroscopic lung lesions and specific quantitative readouts of lung fibrosis (such as the hydroxyproline content and Ashcroft's score) were also reduced by 57% and 47%, respectively [24].

A gain-of-function polymorphism within the promoter region of the *MUC5B* gene (rs35705950) is the strongest genetic risk factor for both familial and sporadic forms of IPF [44]). MUC5B is the main secretory mucin in the superficial epithelium and glands, and its expression is regulated by NF-κB and activating protein-1 [45, 46]. In patients with IPF, over-expression of MUC5B in the distal airways is believed to impair mucociliary clearance and thus lead to excessive lung retention of xenobiotics or endogenous inflammatory debris, which may induce and sustain the development of fibrosis [47]. Notably, GED-0507 was able to restore MUC5B overexpression in the lung of mice receiving BLM.

The main objective of our study was to demonstrate GED-0507's antifibrotic effects *in vitro* on lung epithelial cells and fibroblasts and *in vivo* in a mouse model of experimentally-induced pulmonary fibrosis. We also compared GED-0507 with Pirf and Nint, the two drugs approved for the treatment of IPF. Our choice of the dose levels of GED-0507, Pirf and Nint used here was based on (i) a dose-response evaluation in A549/MRC-5 cell lines and primary HLFs, (ii) *in vivo* data in medical databases on the optimal dosages of Pirf and Nint in BLM-induced lung fibrosis [48–53], and (iii) the dose level of 100 mg/Kg for GED-0507 used in toxicological studies of animals. Chronic administration of increasing concentrations of GED-0507 for 26 days in rats enabled definition of the "no observed adverse effect level" (NOAEL) as 500 mg/Kg/day [54]. In line with the FDA's draft guidelines on dose conversion between animals and humans, the human equivalent dose for GED-0507 is 81 mg/kg/day (based on body surface area), with a maximum human recommended starting dose of 8 mg/kg (the human equivalent dose divided by a safety factor of 10). In a phase IIb clinical trial in inflammatory bowel disease, GED was administered at a dose of 8 mg/kg/day; with a conversion factor of 0.08, this corresponds to 100 mg/Kg/day in the mouse. Based on the same conversion criteria, we administered Pirf and Nint at doses of 400 mg/Kg/day and 60 mg/kg/day, respectively. These are the most commonly used doses in murine models of lung fibrosis and correspond to the US Food and Drug Administration's recommended daily dose for the treatment of patients with IPF (2403 mg/d for Pirf and 300 mg/d for Nint) [55]. When evaluated under the same

conditions, GED-0507 displayed more pronounced antifibrotic activity *in vitro* and *in vivo* than Pirf and Nint for most biomarkers associated with alveolar epithelial cell dysfunction, the EMT, and ECM remodeling.

Our study had several limitations. Firstly, we used A549 cells. Although a number of studies have reported on the use of A549 cells as a model of human alveolar epithelial cells [56], GED-0507's antifibrotic properties need to be confirmed in other cell types, such as alveolar epithelial cells or small airway epithelial cells. Secondly, since one of the features of the BLM model is loss of epithelium, it may be difficult to distinguish between the EMT and loss of epithelium. However, we observed a clear fibrotic profile 28 days after BLM administration. In this regard, a number of studies in mice have shown that BLM administration can induce the EMT [57–59]. Lastly, the mechanisms by which GED-0507-induced modulation of PPAR-γ signaling attenuates lung fibrosis remain to be elucidated.

In conclusion, we provided further evidence of the antifibrotic effects of GED-0507 by demonstrating the compound's ability to modulate several fibrosis pathways in BLM-induced pulmonary fibrosis and in TGFβ-exposed lung epithelial cells and fibroblasts.

GED-0507 has displayed a very favorable safety and tolerability profile in both preclinical and clinical studies. The compound's preclinical safety profile derives from pharmacology studies in rats and dogs, chronic toxicity studies (with up to 26 weeks of repeated-dose oral administration) in rats and 39 weeks in dogs), embryo-fetal development toxicity studies in rats and rabbits, and genotoxicity studies. No effects were observed on either cardiovascular parameters in dogs or nervous and respiratory function in rats at doses up to 2000 mg/kg (the NOAEL). GED-0507 has also proven to be safe and well tolerated in patients with ulcerative colitis at doses of 160 mg/day and 320 mg/day for 8 consecutive weeks. Specifically, no clinically meaningful abnormalities in laboratory tests (hematology, biochemistry, and urine analyses), vital signs, physical findings, or the ECG occurred in any of the subjects during the study period.

GED-0507's potential mechanisms of action of GED-0507 are represented in S3 Fig. GED-0507 is now ready to enter a Phase Ib trial in patients with IPF.

Supporting information

S1 Fig. Outline of experimental design for (a) preventive and (b) curative treatments.
(TIF)

S2 Fig. GED does not show cytotoxic effects in A549 and MRC-5 cell lines and in HLF. Cell viability assay in response to growing concentrations of GED, Pirf and Nint in (a) A549, (b) MRC-5 and (c) HLF cells. Data are expressed as mean of fold changes ± SEM; * = p< 0.05; ** = p< 0.01; *** = p< 0.001.
(TIF)

S3 Fig. Schematic pathophysiology of pulmonary fibrosis. The onset of fibrotic process in lung begins from repeated injuries which lead to inflammatory response, via the activation of the NFκB pathway and consequent release of pro-inflammatory cytokines. Uncontrolled over-production of further cytokines and growth factors, among which TGFβ, induces the succession of a series of reversible cellular processes which culminate in lung fibrosis. Those processes are schematically represented in the figure and include: death of Type I alveolar epithelial cell (AEC), proliferation of Type II alveolar epithelial cells which undergo the epithelial-mesenchymal transition (EMT) and a consequent failure of re-epithelialization, fibroblasts recruitment and proliferation, myofibroblasts activation, ECM deposition and MUC5B

production.
(TIF)

S1 Table. Mouse primer sequences for quantitative RT-PCR.
(PDF)

S2 Table. Human primer sequences for quantitative RT-PCR.
(PDF)

S1 Data.
(PDF)

Author Contributions

Conceptualization: Silvia Speca, Philippe Chavatte, Pierre Desreumaux, Paolo Spagnolo.

Data curation: Silvia Speca, Pierre Desreumaux, Paolo Spagnolo.

Formal analysis: Silvia Speca.

Investigation: Silvia Speca.

Methodology: Caroline Dubuquoy, Christel Rousseaux.

Project administration: Pierre Desreumaux, Paolo Spagnolo.

Supervision: Paolo Spagnolo.

Validation: Philippe Chavatte, Pierre Desreumaux, Paolo Spagnolo.

Visualization: Paolo Spagnolo.

Writing – original draft: Silvia Speca, Pierre Desreumaux, Paolo Spagnolo.

Writing – review & editing: Silvia Speca, Pierre Desreumaux, Paolo Spagnolo.

References

1. Dubuquoy L, Dharancy S, Nutten S, Pettersson S, Auwerx J, Desreumaux P. Role of peroxisome proliferator-activated receptor gamma and retinoid X receptor heterodimer in hepatogastroenterological diseases. Lancet. 2002 Nov 2; 360(9343):1410–8. https://doi.org/10.1016/S0140-6736(02)11395-X PMID: 12424006.

2. Fumery M, Speca S, Langlois A, Davila A-M, Dubuquoy C, Grauso M, et al. Peroxisome proliferator-activated receptor gamma (PPARγ) regulates lactase expression and activity in the gut. EMBO Mol Med. 2017; 9(11):1471–81. https://doi.org/10.15252/emmm.201707795 PMID: 28947679; PMCID: PMC5666307.

3. Speca S, Rousseaux C, Dubuquoy C, Rieder F, Vetuschi A, Sferra R et al. Novel PPARγ Modulator GED-0507-34 Levo Ameliorates Inflammation-driven Intestinal Fibrosis.—PubMed—NCBI. Inflamm Bowel Dis. 2016 Feb; 22(2):279–92. https://doi.org/10.1097/MIB.0000000000000618 PMID: 26535766; PMCID: PMC4718865.

4. Pirat C, Farce A, Lebègue N, Renault N, Furman C, Millet R et al. Targeting peroxisome proliferator-activated receptors (PPARs): development of modulators. J Med Chem. 2012 May 10; 55(9):4027–61. https://doi.org/10.1021/jm101360s PMID: 22260081.

5. Rosenbloom J, Macarak E, Piera-Velazquez S, Jimenez SA. Human Fibrotic Diseases: Current Challenges in Fibrosis Research. Methods Mol Biol. 2017; 1627:1–23. https://doi.org/10.1007/978-1-4939-7113-8_1 PMID: 28836191.

6. Wijsenbeek M, Cottin V. Spectrum of Fibrotic Lung Diseases. N Engl J Med. 2020 Sep 3; 383(10):958–68. https://doi.org/10.1056/NEJMra2005230 PMID: 32877584.

7. Martinez FJ, Lederer DJ. Focus on Idiopathic Pulmonary Fibrosis. Chest. 2018 Oct; 154(4):978–9. https://doi.org/10.1016/j.chest.2018.08.1021 PMID: 30290930.

8. Ley B, Collard HR, King TE. Clinical course and prediction of survival in idiopathic pulmonary fibrosis. Am J Respir Crit Care Med. 2011 Feb 15; 183(4):431–40. https://doi.org/10.1164/rccm.201006-0894CI PMID: 20935110.

9. Raghu G, Remy-Jardin M, Myers JL, Richeldi L, Ryerson CJ, Lederer DJ et al. Diagnosis of Idiopathic Pulmonary Fibrosis. An Official ATS/ERS/JRS/ALAT Clinical Practice Guideline. Am J Respir Crit Care Med. 2018 Sep; 198(5):e44–68. https://doi.org/10.1164/rccm.201807-1255ST PMID: 30168753.

10. King TE, Bradford WZ, Castro-Bernardini S, Fagan EA, Glaspole I, Glassberg MK et al. A phase 3 trial of pirfenidone in patients with idiopathic pulmonary fibrosis. N Engl J Med. 2014 May 29; 370(22):2083–92. https://doi.org/10.1056/NEJMoa1402582 PMID: 24836312.

11. Noble PW, Albera C, Bradford WZ, Costabel U, Glassberg MK, Kardatzke D et al. Pirfenidone in patients with idiopathic pulmonary fibrosis (CAPACITY): two randomised trials. Lancet. 2011 May 21; 377(9779):1760–9. https://doi.org/10.1016/S0140-6736(11)60405-4 PMID: 21571362.

12. Richeldi L, du Bois RM, Raghu G, Azuma A, Brown KK, Costabel U et al. Efficacy and safety of nintedanib in idiopathic pulmonary fibrosis. N Engl J Med. 2014 May 29; 370(22):2071–82. https://doi.org/10.1056/NEJMoa1402584 PMID: 24836310

13. Galli JA, Pandya A, Vega-Olivo M, Dass C, Zhao H, Criner GJ. Pirfenidone and nintedanib for pulmonary fibrosis in clinical practice: Tolerability and adverse drug reactions. Respirology. 2017; 22 (6):1171–8. https://doi.org/10.1111/resp.13024 Epub 2017 Mar 20. PMID: 28317233.

14. Spagnolo P, Kropski JA, Jones MG, Lee JS, Rossi G, Karampitsakos T et al. Idiopathic pulmonary fibrosis: Disease mechanisms and drug development. Pharmacol Ther. 2020 Dec 24; 222:107798. https://doi.org/10.1016/j.pharmthera.2020.107798 Epub ahead of print. PMID: 33359599.

15. Wolters PJ, Collard HR, Jones KD. Pathogenesis of idiopathic pulmonary fibrosis. Annu Rev Pathol. 2014; 9:157–79. https://doi.org/10.1146/annurev-pathol-012513-104706 PMID: 24050627; PMCID: PMC4116429.

16. Rehan VK, Dargan-Batra SK, Wang Y, Cerny L, Sakurai R, Santos J et al. A paradoxical temporal response of the PTHrP/PPARgamma signaling pathway to lipopolysaccharide in an in vitro model of the developing rat lung. Am J Physiol Lung Cell Mol Physiol. 2007 Jul; 293(1):L182–190. https://doi.org/10.1152/ajplung.00319.2006 Epub 2007 Apr 13. PMID: 17435078.

17. Malur A, Mohan A, Barrington RA, Leffler N, Malur A, Muller-Borer B et al. Peroxisome Proliferator-activated Receptor-γ Deficiency Exacerbates Fibrotic Response to Mycobacteria Peptide in Murine Sarcoidosis Model. Am J Respir Cell Mol Biol. 2019 Aug; 61(2):198–208. https://doi.org/10.1165/rcmb.2018-0346OC PMID: 30741559; PMCID: PMC6670028.

18. Sime PJ. The antifibrogenic potential of PPARgamma ligands in pulmonary fibrosis. J Investig Med. 2008 Feb; 56(2):534–8. https://doi.org/10.2310/JIM.0b013e31816464e9 PMID: 18317437.

19. Bellaye P-S, Kolb M. Why do patients get idiopathic pulmonary fibrosis? Current concepts in the pathogenesis of pulmonary fibrosis. BMC Med. 2015 Sep 24; 13:176. https://doi.org/10.1186/s12916-015-0412-6 PMID: 26400687; PMCID: PMC4581472.

20. Lehtonen ST, Veijola A, Karvonen H, Lappi-Blanco E, Sormunen R, Korpela S et al. Pirfenidone and nintedanib modulate properties of fibroblasts and myofibroblasts in idiopathic pulmonary fibrosis. Respir Res. 2016 Feb 4; 17:14. https://doi.org/10.1186/s12931-016-0328-5 PMID: 26846335; PMCID: PMC4743320.

21. Junqueira LC, Bignolas G, Brentani RR. Picrosirius staining plus polarization microscopy, a specific method for collagen detection in tissue sections. Histochem J. 1979 Jul; 11(4):447–55. https://doi.org/10.1007/BF01002772 PMID: 91593.

22. Trackman PC, Saxena D, Bais MV. TGF-β1- and CCN2-Stimulated Sirius Red Assay for Collagen Accumulation in Cultured Cells. Methods Mol Biol. 2017; 1489:481–5. https://doi.org/10.1007/978-1-4939-6430-7_39 PMID: 27734398.

23. Jensen EC. Quantitative analysis of histological staining and fluorescence using ImageJ. Anat Rec (Hoboken). 2013 Mar; 296(3):378–81. https://doi.org/10.1002/ar.22641 Epub 2013 Feb 4. PMID: 23382140.

24. Speca S, Dubuquoy C, Rousseaux C, Chavatte P, Desreumaux P, Spagnolo P. GED-0507 is a novel potential antifibrotic treatment option for pulmonary fibrosis. Cell Mol Immunol. 2020 Mar 12; 2020 Dec; 17(12):1272–1274. https://doi.org/10.1038/s41423-020-0394-y PMID: 32203183; PMCID: PMC7784849.

25. Mouratis MA, Aidinis V. Modeling pulmonary fibrosis with bleomycin. Curr Opin Pulm Med. 2011 Sep; 17(5):355–61. https://doi.org/10.1097/MCP.0b013e328349ac2b PMID: 21832918.

26. Henderson NC, Rieder F, Wynn TA. Fibrosis: from mechanisms to medicines. Nature. 2020 Nov; 587 (7835):555–66. https://doi.org/10.1038/s41586-020-2938-9 PMID: 33239795; PMCID: PMC8034822.

27. Iyer SN, Gurujeyalakshmi G, Giri SN. Effects of pirfenidone on transforming growth factor-beta gene expression at the transcriptional level in bleomycin hamster model of lung fibrosis. J Pharmacol Exp Ther. 1999 Oct; 291(1):367–73. PMID: 10490926.

28. Wollin L, Wex E, Pautsch A, Schnapp G, Hostettler KE, Stowasser S et al. Mode of action of nintedanib in the treatment of idiopathic pulmonary fibrosis. Eur Respir J. 2015 May; 45(5):1434–45. https://doi.org/10.1183/09031936.00174914 PMID: 25745043; PMCID: PMC4416110.

29. Rangarajan S, Kurundkar A, Kurundkar D, Bernard K, Sanders YY, Ding Q et al. Novel Mechanisms for the Antifibrotic Action of Nintedanib. Am J Respir Cell Mol Biol. 2016 Jan; 54(1):51–9. https://doi.org/10.1165/rcmb.2014-0445OC PMID: 26072676; PMCID: PMC4742925.

30. Wynn TA. Cellular and molecular mechanisms of fibrosis. J Pathol. 2008 Jan; 214(2):199–210. https://doi.org/10.1002/path.2277 PMID: 18161745; PMCID: PMC2693329.

31. Tyagi S, Gupta P, Saini AS, Kaushal C, Sharma S. The peroxisome proliferator-activated receptor: A family of nuclear receptors role in various diseases. J Adv Pharm Technol Res. 2011; 2(4):236–40. https://doi.org/10.4103/2231-4040.90879 PMID: 22247890; PMCID: PMC3255347.

32. Milam JE, Keshamouni VG, Phan SH, Hu B, Gangireddy SR, Hogaboam CM et al. PPAR-gamma agonists inhibit profibrotic phenotypes in human lung fibroblasts and bleomycin-induced pulmonary fibrosis. Am J Physiol Lung Cell Mol Physiol. 2008 May; 294(5):L891–901. https://doi.org/10.1152/ajplung.00333.2007 PMID: 18162602; PMCID: PMC5926773.

33. Burgess HA, Daugherty LE, Thatcher TH, Lakatos HF, Ray DM, Redonnet M et al. PPARgamma agonists inhibit TGF-beta induced pulmonary myofibroblast differentiation and collagen production: implications for therapy of lung fibrosis. Am J Physiol Lung Cell Mol Physiol. 2005 Jun; 288(6):L1146–1153. https://doi.org/10.1152/ajplung.00383.2004 Epub 2005 Feb 25. PMID: 15734787.

34. Genovese T, Cuzzocrea S, Di Paola R, Mazzon E, Mastruzzo C, Catalano P et al. Effect of rosiglitazone and 15-deoxy-Delta12,14-prostaglandin J2 on bleomycin-induced lung injury. Eur Respir J. 2005 Feb; 25(2):225–34. https://doi.org/10.1183/09031936.05.00049704 PMID: 15684285.

35. Aoki Y, Maeno T, Aoyagi K, Ueno M, Aoki F, Aoki N et al. Pioglitazone, a peroxisome proliferator-activated receptor gamma ligand, suppresses bleomycin-induced acute lung injury and fibrosis. Respiration. 2009; 77(3):311–9. https://doi.org/10.1159/000168676 PMID: 18974632.

36. Samah M, El-Aidy AE-R, Tawfik MK, Ewais MMS. Evaluation of the antifibrotic effect of fenofibrate and rosiglitazone on bleomycin-induced pulmonary fibrosis in rats. Eur J Pharmacol. 2012 Aug 15; 689(1–3):186–93. https://doi.org/10.1016/j.ejphar.2012.05.026 PMID: 22659583.

37. Mangoni M, Sottili M, Gerini C, Bonomo P, Bottoncetti A, Castiglione F et al. A PPAR-gamma agonist attenuates pulmonary injury induced by irradiation in a murine model. Lung Cancer. 2015 Dec; 90(3):405–9. https://doi.org/10.1016/j.lungcan.2015.11.005 PMID: 26791799.

38. Huang TH-W, Razmovski-Naumovski V, Kota BP, Lin DS-H, Roufogalis BD. The pathophysiological function of peroxisome proliferator-activated receptor-gamma in lung-related diseases. Respir Res. 2005 Sep 9; 6:102. https://doi.org/10.1186/1465-9921-6-102 PMID: 16153299; PMCID: PMC1242255.

39. Kung J, Henry RR. Thiazolidinedione safety. Expert Opin Drug Saf. 2012 Jul; 11(4):565–79. https://doi.org/10.1517/14740338.2012.691963 PMID: 22616948.

40. Bertin B, Dubuquoy L, Colombel J-F, Desreumaux P. PPAR-gamma in ulcerative colitis: a novel target for intervention. Curr Drug Targets. 2013 Nov; 14(12):1501–7. https://doi.org/10.2174/13894501113149990162 PMID: 23651165.

41. Mastrofrancesco A, Kovacs D, Sarra M, Bastonini E, Cardinali G, Aspite N, et al. Preclinical studies of a specific PPARγ modulator in the control of skin inflammation. J Invest Dermatol. 2014 Apr; 134(4):1001–11. https://doi.org/10.1038/jid.2013.448 PMID: 24166135.

42. Di Gregorio J, Sferra R, Speca S, Vetuschi A, Dubuquoy C, Desreumaux P et al. Role of glycogen synthase kinase-3β and PPAR-γ on epithelial-to-mesenchymal transition in DSS-induced colorectal fibrosis. PLoS One. 2017 Feb; 12(2):e0171093. https://doi.org/10.1371/journal.pone.0171093 PMID: 28207769; PMCID: PMC5313173.

43. Vetuschi A, Pompili S, Gaudio E, Latella G, Sferra R. PPAR-γ with its anti-inflammatory and anti-fibrotic action could be an effective therapeutic target in IBD. Eur Rev Med Pharmacol Sci. 2018; 22(24):8839–48. https://doi.org/10.26355/eurrev_201812_16652 PMID: 30575926.

44. Schwartz DA. PMID: 28066036. Trans Am Clin Climatol Assoc. 2016; 127:34–45. PMCID: PMC5216513.

45. Fujisawa T, Chang MM-J, Velichko S, Thai P, Hung L-Y, Huang F et al. NF-κB mediates IL-1β- and IL-17A-induced MUC5B expression in airway epithelial cells. Am J Respir Cell Mol Biol. 2011 Aug; 45(2):246–52. https://doi.org/10.1165/rcmb.2009-0313OC PMID: 20935193; PMCID: PMC3175554.

46. Lee J-W, Kim YI, Im C-N, Kim SW, Kim SJ, Min S et al. Grape Seed Proanthocyanidin Inhibits Mucin Synthesis and Viral Replication by Suppression of AP-1 and NF-κB via p38 MAPKs/JNK Signaling

Pathways in Respiratory Syncytial Virus-Infected A549 Cells. J Agric Food Chem. 2017 Jun 7; 65 (22):4472–83. https://doi.org/10.1021/acs.jafc.7b00923 Epub 2017 May 23. PMID: 28502165.

47. Hancock LA, Hennessy CE, Solomon GM, Dobrinskikh E, Estrella A, Hara N et al. Muc5b overexpression causes mucociliary dysfunction and enhances lung fibrosis in mice. Nat Commun. 2018 Dec 18;9. https://doi.org/10.1038/s41467-017-01881-x PMID: 29339724; PMCID: PMC6299094.

48. Tanaka K-I, Azuma A, Miyazaki Y, Sato K, Mizushima T. Effects of lecithinized superoxide dismutase and/or pirfenidone against bleomycin-induced pulmonary fibrosis. Chest. 2012 Oct; 142(4):1011–9. https://doi.org/10.1378/chest.11-2879 PMID: 22459774.

49. Kakugawa T, Mukae H, Hayashi T, Ishii H, Abe K, Fujii T et al. Pirfenidone attenuates expression of HSP47 in murine bleomycin-induced pulmonary fibrosis. Eur Respir J. 2004 Jul; 24(1):57–65. https://doi.org/10.1183/09031936.04.00120803 PMID: 15293605.

50. Lv X, Wang X, Li K, Wang Z, Li Z, Lv Q et al. Rupatadine protects against pulmonary fibrosis by attenuating PAF-mediated senescence in rodents. PLoS ONE. 2013; 8(7):e68631. https://doi.org/10.1371/journal.pone.0068631 PMID: 23869224; PMCID: PMC3711902.

51. Li L-F, Kao K-C, Liu Y-Y, Lin C-W, Chen N-H, Lee C-S et al. Nintedanib reduces ventilation-augmented bleomycin-induced epithelial-mesenchymal transition and lung fibrosis through suppression of the Src pathway. J Cell Mol Med. 2017 Nov; 21(11):2937–49. https://doi.org/10.1111/jcmm.13206 PMID: 28598023; PMCID: PMC5661114.

52. Shi Q, Liu X, Bai Y, Cui C, Li J, Li Y et al. In vitro effects of pirfenidone on cardiac fibroblasts: proliferation, myofibroblast differentiation, migration and cytokine secretion. PLoS ONE. 2011; 6(11):e28134. https://doi.org/10.1371/journal.pone.0028134 PMID: 22132230; PMCID: PMC3223242.

53. Hostettler KE, Zhong J, Papakonstantinou E, Karakiulakis G, Tamm M, Seidel P et al. Anti-fibrotic effects of nintedanib in lung fibroblasts derived from patients with idiopathic pulmonary fibrosis. Respir Res. 2014 Dec 12; 15:157. https://doi.org/10.1186/s12931-014-0157-3 PMID: 25496490; PMCID: PMC4273482.

54. U.S. Department of Health and Human Services, Food and Drug Administration, Center for Drug Evaluation and Research (CDER). Guidance for Industry. 2005 Jul; Available from: https://www.fda.gov/media/72309/download

55. Nair AB, Jacob S. A simple practice guide for dose conversion between animals and human. J Basic Clin Pharm. 2016 Mar; 7(2):27–31. https://doi.org/10.4103/0976-0105.177703 PMID: 27057123; PMCID: PMC4804402.

56. Lukaszewicz A, Cwiklinska M, Zarzecki M, Szoka P, Lachowicz J, Holownia A. Cytotoxicity, Oxidative Stress, and Autophagy in Human Alveolar Epithelial Cell Line (A549 Cells) Exposed to Standardized Urban Dust. Adv Exp Med Biol. 2019; 1176:101–8. https://doi.org/10.1007/5584_2019_387 PMID: 31175637.

57. Weng C-M, Li Q, Chen K-J, Xu C-X, Deng M-S, Li T et al. Bleomycin induces epithelial-to-mesenchymal transition via bFGF/PI3K/ESRP1 signaling in pulmonary fibrosis. Biosci Rep. 2020 Jan 31; 40(1). https://doi.org/10.1042/BSR20190756 PMID: 31868203; PMCID: PMC6960066.

58. Qian W, Cai X, Qian Q, Zhang W, Wang D. Astragaloside IV modulates TGF-β1-dependent epithelial-mesenchymal transition in bleomycin-induced pulmonary fibrosis. J Cell Mol Med. 2018 Sep; 22 (9):4354–65. https://doi.org/10.1111/jcmm.13725 PMID: 29971947; PMCID: PMC6111865.

59. Chen K-J, Li Q, Weng C-M, Duan Z-X, Zhang D-D, Chen Z-Q et al. Bleomycin-enhanced alternative splicing of fibroblast growth factor receptor 2 induces epithelial to mesenchymal transition in lung fibrosis. Biosci Rep. 2018 Dec 21; 38(6). https://doi.org/10.1042/BSR20180445 PMID: 30049844; PMCID: PMC6239266.